Parvalbumin interneuron in the ventral hippocampus functions as a discriminator in social memory

Xiaofei Deng[a,b], Lijia Gu[a,b], Nan Sui[a,b], Jianyou Guo[a,b,1], and Jing Liang[a,b,1]

[a]CAS Key Laboratory of Mental Health, Institute of Psychology, Chinese Academy of Sciences, Beijing, China 100101; and [b]Department of Psychology, University of Chinese Academy of Sciences, Beijing, China 100049

Edited by Takao K. Hensch, Harvard University, Cambridge, MA, and accepted by Editorial Board Member Nancy Y. Ip July 1, 2019 (received for review November 13, 2018)

The ability to identify strange conspecifics in societies is supported by social memory, which is vital for gregarious animals and humans. The function of hippocampal principal neurons in social memory has been extensively investigated; however, the nonprincipal neuronal mechanism underlying social memory remains unclear. Here, we first observed parallel changes in the ability for social recognition and the number of parvalbumin interneurons (PVIs) in the ventral CA1 (vCA1) after social isolation. Then, using tetanus toxin-mediated neuronal lesion and optogenetic stimulation approaches, we revealed that vCA1-PVIs specifically engaged in the retrieval stage of social memory. Finally, through the in vivo Ca^{2+} imaging technique, we demonstrated that vCA1-PVIs exhibited higher activities when subjected mice approached a novel mouse than to a familiar one. These results highlight the crucial role of vCA1-PVIs for distinguishing novel conspecifics from other individuals and contribute to our understanding of the neuropathology of mental diseases with social memory deficits.

social memory | hippocampus | interneurons | parvalbumin

Social memory functions are the mind's ability to memorize and identify conspecific individuals, which is essential in social interactions, social hierarchies, reproduction, and species survival (1). Like other types of memory systems, social memory's information processing comprises multiple subcomponents: encoding, consolidation, and retrieval (2, 3). Therefore, there are at least three possible reasons for an inability to recognize familiar conspecifics: 1) failure to encode social information, 2) the acquisition of information without its maintenance, and 3) failure to recall information. Studies on humans and animals have demonstrated hippocampal engagement in different processing stages of episodic memory (2, 4), which is a collection of autobiographical experiences comprising four basic elements: when, where, who, and what. As a component of episodic memory, social memory provides critical information about "who," which has been proven to be closely related to hippocampal function (5–10). Moreover, social memory deficits, common symptoms in such conditions as Alzheimer's disease, schizophrenia, and autism, are associated with hippocampus dysfunction (11–14). Although the roles of hippocampal subfields and principal cells (PCs) in hippocampus formation relevant to social memory have recently attracted considerable attention (6–8), little is known about how hippocampal interneurons and local microcircuits are involved in this cognitive process.

Interneurons display a larger cellular diversity than do PCs. At least 21 different types of interneurons have been identified in the hippocampal CA1 area, which supports distinct neural activity and cognitive processing (15). Among these, a subpopulation of GABAergic interneurons called parvalbumin interneurons (PVIs) or fast-spiking interneurons (FSIs) have attracted considerable attention in the last few years (16–18). This interneuron subtype accounts for 24% of all GABAergic cells in the hippocampal CA1 region (19). It has been shown to be involved in diverse brain functions, including but not limited to the modulation of PCs (16, 18), synaptic plasticity (20, 21), and the generation of network oscillation (22–24). Although existing studies have suggested a possible relationship between hippocampal PVIs and social memory (14, 25), the specific mechanism of PVIs' participation in this unique form of memory is poorly understood.

We conducted a series of experiments to dissect the functional role of hippocampal PVIs in social recognition memory. Firstly, to examine whether hippocampal PVIs are involved in social experience-modulated social memory, we performed a social discrimination test (SDT) and a quantitative analysis of parvalbumin-positive (PV^+) immunofluorescence following social isolation. Later, after selectively blocking the synaptic transmission of hippocampal PVIs with an adeno-associated virus (AAV)-mediated tetanus toxin light chain (TeNT), we confirmed the effects of PVI transmission blockades on social memory. To determine the PVI-mediated processing stage's role in social memory, we applied an optogenetic approach to activate or inhibit PVIs in the familiarization, separation, and recognition procedures of the SDT, which are thought to respectively correspond to the encoding, consolidation, and retrieval stages of social memory. Finally, to elucidate the temporal profiles of hippocampal PVIs during social recognition processing, we recorded the Ca^{2+} activity of PVIs in freely moving mice using a fiber photometry technique. Based on these results, we revealed that PVIs in the CA1 subregion of the ventral hippocampus (vCA1) play a key role in identifying familiar and novel conspecifics by regulating the retrieval of social information.

Results

Impaired Social Recognition Memory Occurring with a Decreased Number of PVIs in the Ventral Hippocampus. Previous studies have demonstrated that social isolation could impair long-term social

Significance

Recent studies have identified the hippocampal projection neurons and related pathways that encode and keep social information about familiar conspecifics. On the other side of the coin, however, the neural mechanism for animals to determine the stranger in a group achieved little attention. Here, we demonstrate that ventral CA1 parvalbumin interneurons (vCA1-PVIs) specifically participated in retrieval of social information, and their excitation is crucial for distinguishing novel from familiar conspecifics. These findings not only highlight the importance of hippocampal interneurons in social memory, but also contribute to establish the relationship between PVIs' deficits and impaired social memory in some psychiatric illnesses.

Author contributions: X.D. and J.L. designed research; X.D., L.G., and J.L. performed research; X.D. and J.L. analyzed data; and X.D., N.S., J.G., and J.L. wrote the paper.

The authors declare no conflict of interest.

This article is a PNAS Direct Submission. T.K.H. is a guest editor invited by the Editorial Board.

[1]To whom correspondence may be addressed. Email: guojy@psych.ac.cn or liangj@psych.ac.cn.

This article contains supporting information online at www.pnas.org/lookup/suppl/doi:10.1073/pnas.1819133116/-/DCSupplemental.

Published online July 29, 2019.

recognition memory (5, 26) and down-regulate PV expression in the cortex (27–29). The changes of PV expression in the hippocampus, however, were inconsistent in the few previously existing studies (27, 30, 31). To examine the relationship between social memory ability and the number of PVIs in the hippocampus, a group of early adolescent mice (postnatal day 28 [P28]) were individually isolated without any form of social interaction for 8 wk (individual-housed [IH]) whereas animals of the same age in the control group were housed together (2 to 5 mice per cage; group-housed [GH]) (*SI Appendix*, Fig. S1*A*). Social memory was quantified using a modified SDT (7, 32), which is a valid test based on the preferred rodent nature for examining interactions with novel conspecifics rather than familiar ones. Mice were subjected to an SDT (Fig. 1*A*) at P88 and a novel object recognition test (NORT) at P90 (*SI Appendix*, Fig. S2*A*); they were then killed 1 wk after the completion of the behavioral tests (at P102).

We found that the IH mice exhibited no difference in sniffing duration between novel and familiar mice in the SDT while GH mice showed a normal preference for novel mice over familiar ones (Fig. 1*C*) (see *SI Appendix*, Table S1 for more details on effect statistics, similarly hereinafter). A significantly lower social discrimination index (SDI) was found in the IH mice than in the GH mice (Fig. 1*D*), indicating that social isolation may impair social recognition. Representative mouse tracks in SDT are shown in Fig. 1*B*. However, social isolation did not affect the mice's performance in the NORT (Fig. 1*E*) or in the object discrimination index (ODI) (Fig. 1*F*). Moreover, the numbers of PV^+ neurons in mouse ventral hippocampus (vHPC) were significantly lower in the IH group than in the GH group (Fig. 1 *G*, *Bottom* and *I*). In contrast, there was no significant difference in PV^+ count in the dorsal hippocampus (dHPC) of the two groups (Fig. 1 *G*, *Top* and *H*). We further calculated the correlation

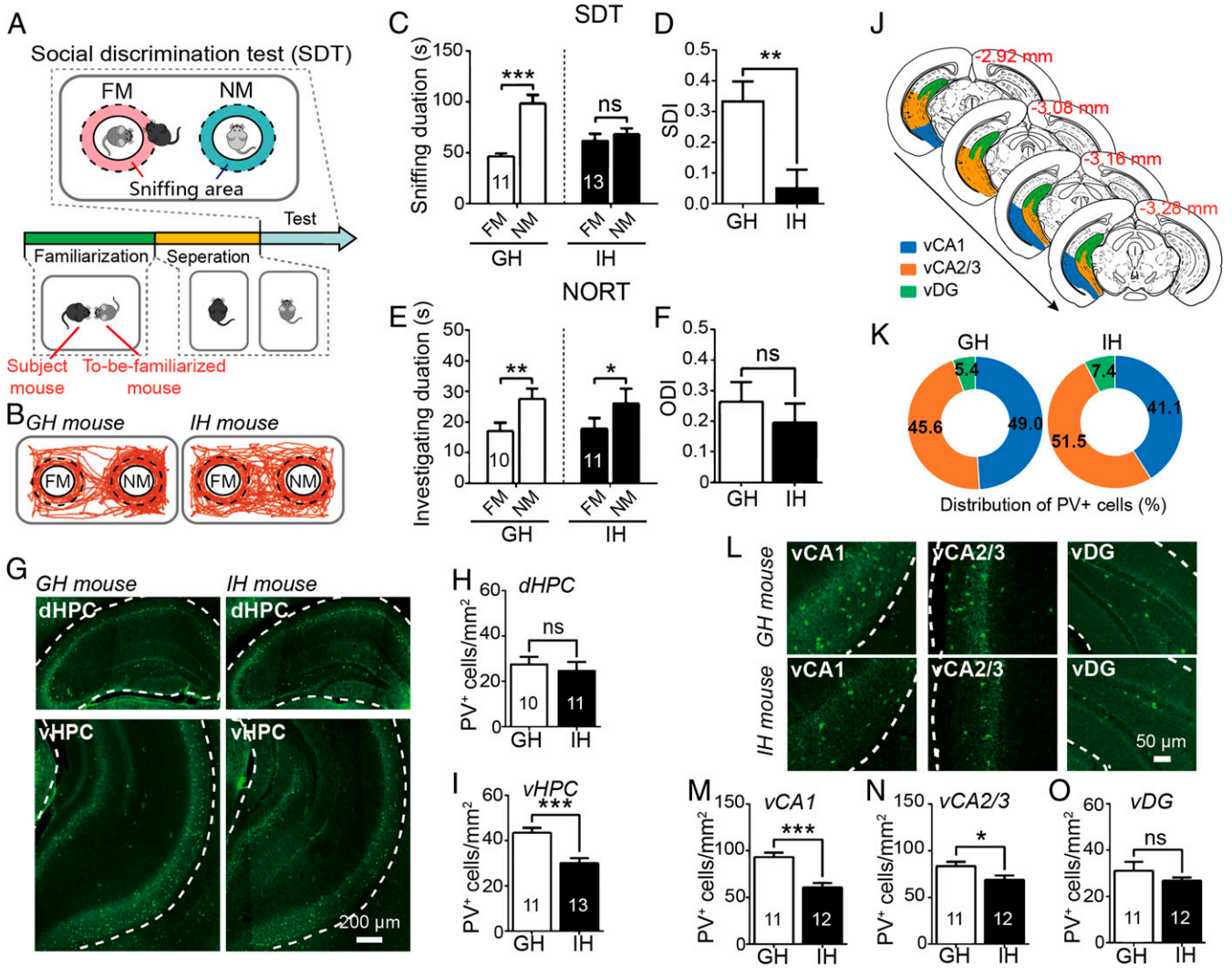

Fig. 1. Impact of 2-mo social isolation on social recognition memory and PV expression in hippocampus. (*A*) Protocol for social discrimination test (SDT). (*B*) Representative mouse tracks during the SDT. FM, familiar mouse; NM, novel mouse. (*C* and *D*) Individual-housed (IH) mice ($n = 13$) exhibited social recognition deficits in SDT while group-housed (GH) mice ($n = 11$) performed SDT normally (*C*); comparison of social discrimination index (SDI) between the GH and the IH mice (*D*). (*E* and *F*) In novel object recognition test (NORT), both groups showed a normal preference for novel object (GH: $n = 10$; IH: $n = 11$) (*E*); no difference was detected in object discrimination index (ODI) between groups (*F*). (*G*) Coronal micrographs showing PV expression in the dHPC (*Top*) and vHPC (*Bottom*). (*H* and *I*) Comparisons of PV^+ counts in the dHPC (GH: $n = 10$; IH: $n = 11$) (*H*) and vHPC (GH: $n = 11$; IH: $n = 13$) (*I*). (*J*) The hippocampal subfields of interest delineation. Blue, vCA1; orange, vCA2/3; green, vDG. (*K*) The distribution of the proportion of PV^+ cells in distinct subfields of vHPC. (*L*) Coronal micrographs showing PV expression in subfields of the vHPC. (*M–O*) Comparisons of PV^+ counts in vCA1 (*M*), vCA2/3 (*N*), and vDG (*O*). GH: $n = 11$; IH: $n = 12$; FM, familiar mouse; NM, novel mouse. The areas of vHPC (*G*) and its subfields (*L*) for analyzing PV^+ counts are outlined by the dashed lines. All data are expressed as mean ± SEM $*P < 0.05$; $**P < 0.01$; $***P < 0.01$; ns: not significant.

coefficient between mouse behavioral performances and PV^+ counts in dHPC and vHPC. A significant positive correlation was found between PV^+ counts in the vHPC (but not the dHPC) and SDI scores (*SI Appendix*, Figs. S1*B* and S2*H*). PV^+ counts in the vHPC or dHPC did not significantly correlate with ODI scores (*SI Appendix*, Figs. S1*C* and S2*I*). Further analyses of the data from the subfields of the vHPCs and dHPCs revealed that the decreasing numbers of PV^+ cells were significant in the vCA1 and vCA2/3 (Fig. 1 *M* and *N*) while they were at the limits of significance in the ventral dentate gyrus (vDG) (Fig. 1*O*). The regions of interest (ROI) delineation is shown in Fig. 1*J* for vHPC. The proportion of PV^+ cells distributed in the subregions of the vHPC also changed after social isolation treatment (Fig. 1*K*). The number of PV^+ cells in the vCA1—but not the vCA2/3 or the vDG—correlated significantly with mice's SDT performances (*SI Appendix*, Fig. S1 *D–F*). We did not separately count the PV^+ cells in the vCA2 and vCA3 because their boundaries could not be easily detected in the vHPC. Full analyses of the dHPC (*SI Appendix*, Fig. S2*B*) revealed no change in proportion of PV^+ cells distribution (*SI Appendix*, Fig. S2*C*) or no correlation between SDI scores and PV^+ cell numbers in any dHPC subfields (*SI Appendix*, Fig. S2 *J–M*) although IH mice showed a PV^+ counts increase in the dDG relative to GH mice (*SI Appendix*, Fig. S2 *D–G*). Additionally, novel object recognition did not appear to be associated with the number of PV^+ cells in any one of the vHPC or dHPC subfields (*SI Appendix*, Figs. S1 *G–I* and S2 *N–Q*). These results suggest that the decline in PV^+ neuron numbers in the vHPC, particularly in the vCA1 subfield, may be partially responsible for synergistic decline in social recognition abilities after social isolation.

To further identify whether or not this alteration in the number of vCA1 PV^+ neurons could be repaired through social recovery, we examined the PV^+ cell counts in the vCA1 following the reexposure of socially isolated mice to the social environments. The results indicated that the diminished quantity of PV^+ neurons in the vCA1 caused by social isolation could be partially restored after 2 wk of social regroup housing; impaired social recognition was also somewhat recovered after this intervention (*SI Appendix*, Fig. S3). These observations suggest that social isolation may disrupt PV expression in existing PVIs rather than cause reductions in PVI numbers, as demonstrated by previous studies (27, 31). It is also suggested that 2 wk of social exposure in adulthood may be unable to entirely rectify the reduced PV expression and damaged social recognition resulting from 2 mo of social isolation during adolescence.

Functionally Removing PVIs from the vCA1 Induced a Deficit in Social Recognition. To clarify whether or not the hippocampal PVIs are engaged in social memory, we selectively blocked the synaptic output of PVIs in the vCA1s and dorsal CA1 (dCA1) in PV-Cre mice with Cre-dependent AAV-carrying GFP-tagged TeNT (AAV-DIO-CMV-TeNT-GFP) (Fig. 2 *A* and *B*). The mice's SDTs were conducted 4 wk after viral injections and 24 h after familiarization with a juvenile mouse before a 30-min separation. The mice treated with TeNT showed no significant difference in investigating duration between novel and familiar mice while the control group exhibited a normal preference for novel mice over familiar ones (Fig. 2*C*). The TeNT group showed significantly lower SDI scores than those of the control group (Fig. 2*D*). By contrast, the same dCA1 manipulation had no effect on the sniffing duration around the novel and familiar mice (*SI Appendix*, Fig. S4 *A* and *B*), and both groups had the similar SDI scores (*SI Appendix*, Fig. S4*C*). To examine the contribution of other subpopulations of GABAergic interneurons to social memory, we injected AAV-DIO-CMV-TeNT-GFP into the vCA1 of somatostatin (SOM)-Cre mice; this transgenic mouse strain specifically expresses Cre proteins in SOM interneurons (SOMIs). Interestingly, the data showed no deficits in the SDT (Fig. 2 *E* and *F*), suggesting that SOMI-selective inactivation in vCA1s had no impact on social memory. These results demonstrate that the PVIs in the vCA1 may be specifically involved in social memory.

Alongside social recognition analyses, we performed NORTs on PV-TeNT mice to determine if the chronic inactivation of vCA1-PVIs could also influence other forms of recognition memory. The results showed that the PV-TeNT group was incapable of discriminating between novel and familiar objects, and the ODI scores in the TeNT group were significantly lower than those of the GFP control group (*SI Appendix*, Fig. S4*D*). Thus, it appears that the impact of the functional absence of vCA1-PVIs on recognition memory is not restricted to social recognition.

We additionally conducted a three-chamber sociability test in PV-TeNT mice to reassess the role of PVIs in social memory and to test whether PVIs are also involved in the regulation of social motivation (Fig. 2*G*). As shown in Fig. 2*H*, during the social interaction session, no significant difference in the time spent in social chambers was noted between TeNT and GFP mice, and no significant difference was observed in the social interaction index between these groups (Fig. 2*I*). In the social novelty session (a novel mouse was introduced into the nonsocial chamber), however, PV-TeNT mice displayed no preference for the novel mouse chamber (Fig. 2*J*) and had significantly lower social novelty index scores than did the control (Fig. 2*K*), which was consistent with the SDT results.

To examine the effects of the disruption of vCA1-PVI inhibition on anxiety, locomotion, and sensorimotor gating, we conducted elevated plus maze (EPM), open field, and prepulse inhibition (PPI) tests. The PV-TeNT mice spent significantly more time than the other mice in the open arms of the EPM and in the center zone of the open field (*SI Appendix*, Fig. S4*E*), reflecting reduced anxiety levels. But no significant differences in total traveled distance or mean speed were noted between these mice and the control group (*SI Appendix*, Fig. S4*F*). The calculated PPI rates of PV-TeNT mice at different prepulse intensities (66, 70, 74, and 78 dB) were not significantly different from those of the control mice (*SI Appendix*, Fig. S4*G*).

Optogenetic Stimulation of vCA1-PVIs Disrupted Only Social Memory Retrieval (Not Encoding or Consolidation). To investigate the particular stage of the social memory process mediated by hippocampal PVIs, we bilaterally injected Cre-dependent AAVs to express channelrhodopsin-2 (ChR2) or enhanced halorhodopsin (NpHR) in PV-Cre mice and implanted optical fibers into their vCA1s (Fig. 3*A*). A 473-nm blue laser (10 ms per pulse, 8 Hz, 15 mW) or a 589-nm yellow laser (constant, 10 mW) was used to optogenetically manipulate PVI activity. We first tested the effect of optogenetic stimulation on social memory's retrieval stage. As shown in Fig. 3*B*, during the recognition session, optogenetic stimulation was delivered for 5 min. According to a comparison with their respective control groups, the PV-ChR2 mice were found to spend a similar amount of time investigating both target (one novel mouse, one familiar mouse) mice (Fig. 3*C*) while PV-NpHR mice appeared to prefer to approach the novel mouse over the familiar one (Fig. 3*E*). Nevertheless, both the optogenetic activation and inhibition of vCA1-PVIs resulted in significantly lower SDI scores than those in their respective control groups (Fig. 3 *D* and *F*). The same PV-ChR2 and PV-NpHR mice exhibited a normal SDT performance (*SI Appendix*, Fig. S5 *A* and *C*) and got higher SDI scores when they did not receive laser manipulation than when they did (*SI Appendix*, Fig. S5 *B* and *D*). These results indicate that both the excitation and inhibition of vCA1-PVIs can alter social memory recall.

To determine whether social recognition can also be disrupted by regulating vCA1-PVIs when a to-be-recognized mouse is fully familiarized, we replaced mice familiar to the subject mice with the mice housed together with the subject mice for over 2 wk during the SDT (their so-called roommates). Intriguingly, in this condition, PV-specific excitation did not influence social discrimination (*SI*

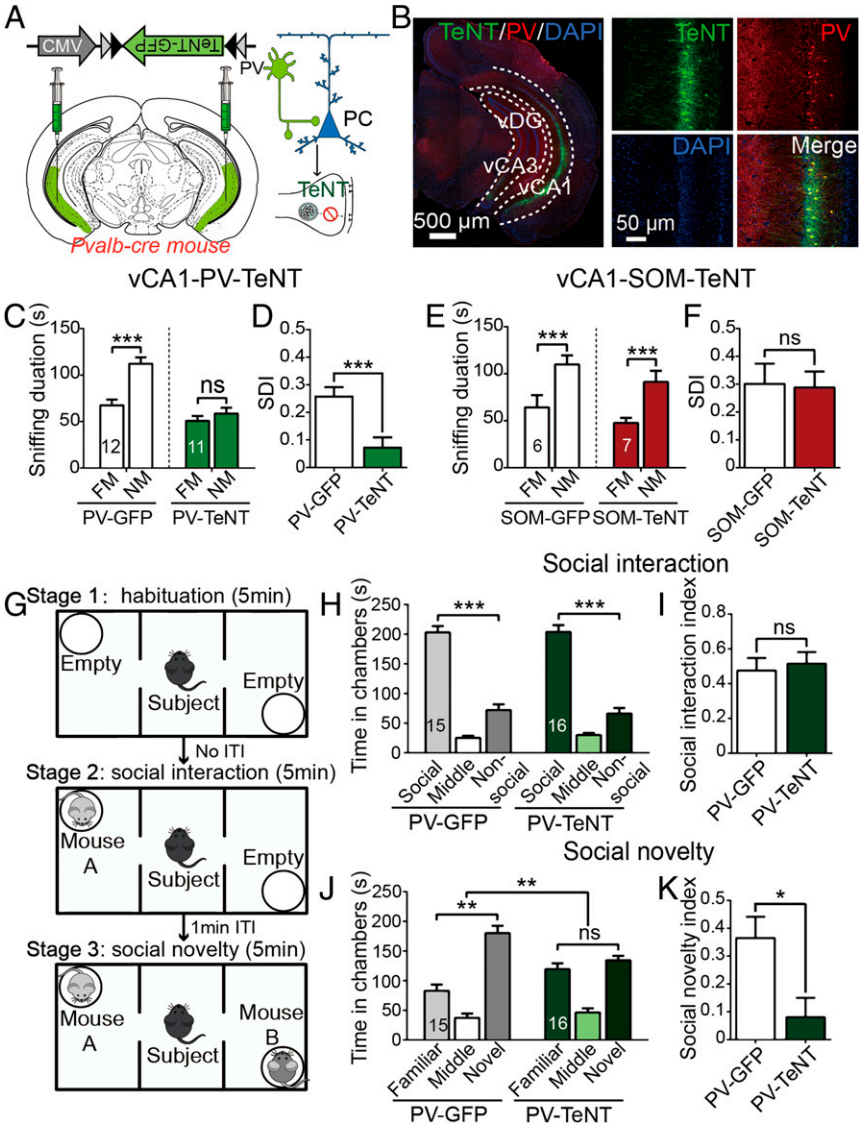

Fig. 2. Functional absence of vCA1-PVIs by TeNT impaired social memory. (*A*) AAV-CMV-DIO-TeNT-GFP was injected into the vCA1 of PV-Cre mice. TeNT could selectively block transmitter release in PVIs. (*B*) Representative coronal sections of a vCA1-PV-TeNT mouse, which were stained with anti-GFP (green), PV (red), and DAPI (blue). (*C* and *E*) Total duration in sniffing area during the SDT observed in PV-GFP ($n = 12$) and PV-TeNT mice ($n = 11$) (*C*) and SOM-GFP ($n = 6$) and SOM-TeNT ($n = 7$) mice (*E*). (*D* and *F*) Comparisons of SDI in experiment of PV-TeNT (*D*) and SOM-TeNT (*F*). (*G*) Protocol for 3-chamber sociability test. (*H* and *I*) During social interaction session, both groups spent more time in the social than nonsocial chamber (GFP: $n = 15$; TeNT: $n = 16$) (*H*); comparison of social interaction index (*I*). (*J* and *K*) During social novelty session, PV-TeNT mice did not display a preference for novel mouse (*J*); comparison of social novelty index (*K*). FM, familiar mouse; NM, novel mouse. All data are expressed as mean ± SEM. $^{*}P < 0.05$; $^{**}P < 0.01$; $^{***}P < 0.001$; ns, not significant.

Appendix, Fig. S5 *E* and *F*). It is possible that a 2-wk familiarization period enables subject mice to recognize familiar mice by information other than odor, such as appearance or vocalizations, which is less reliant on vCA1. Note that PV-TeNT mice were incapable of discriminating between the novel mice and their own roommates (*SI Appendix*, Fig. S5 *G* and *H*). Thus, it seems that chronic PVI inactivation by TeNT has a broad and longstanding impact on social memory.

To examine whether the acute manipulation of the vCA1-PVIs could affect the discrimination of nonsocial stimuli, an optogenetic laser was delivered during the NORT. We determined that neither activation nor inhibition of PVIs impaired the novel object recognition (*SI Appendix*, Fig. S5 *I* and *K*). No difference in ODI score between each optogenetic group and its respective control group was detected (*SI Appendix*, Fig. S5 *J* and *L*). The TeNT experiments' inconsistency with NORT results suggests that chronic and acute manipulations of vCA1-PVIs may act on neural systems and behaviors in different manners. In the open field test, no change was detected in the total traveled distance or total travel time in the center zone (*SI Appendix*, Fig. S5 *M–P*), suggesting that the acute stimulation of PVIs does not affect locomotion or anxiety.

Subsequently, to examine whether PVIs in the vCA1 are involved in social memory's encoding stage, optogenetic stimulation was delivered during the SDT's familiarization stage. To focus on this processing stage, we modified the SDT procedure slightly according to the study by Engelmann et al. (32). The familiarization session in this procedure lasted 10 min, during which optogenetic stimulation was delivered (Fig. 3*G*). We performed the SDT after a separation period of 24 h and found that neither the activation nor the inhibition of PVIs in the vCA1 disrupted the mice's ability to socially discriminate between novel and familiar mice (Fig. 3 *H* and *J*). The SDI scores of ChR2 and NpHR mice were not significantly different from those of their controls (Fig. 3 *I* and *K*), indicating the presence of an intact encoding ability for social information processing.

To explore the potential participation of vCA1-PVIs in the consolidation stage, we optogenetically stimulated the PVIs during the SDT's separation session. Each subject received a 10-min optogenetic stimulation once per test, and this was repeated four times at different time markers (30, 60, 180, and 360 min following a single 10-min social interaction with the to-be-familiarized mice). The SDT was performed 24 h after familiarization (Fig. 3*L*). The data showed that, regardless of when the optogenetic stimulation was delivered, no significant difference in SDI was observed between the ChR2 and mCherry (mCh) mice (Fig. 3*M*). Similarly, no change in SDI was found in

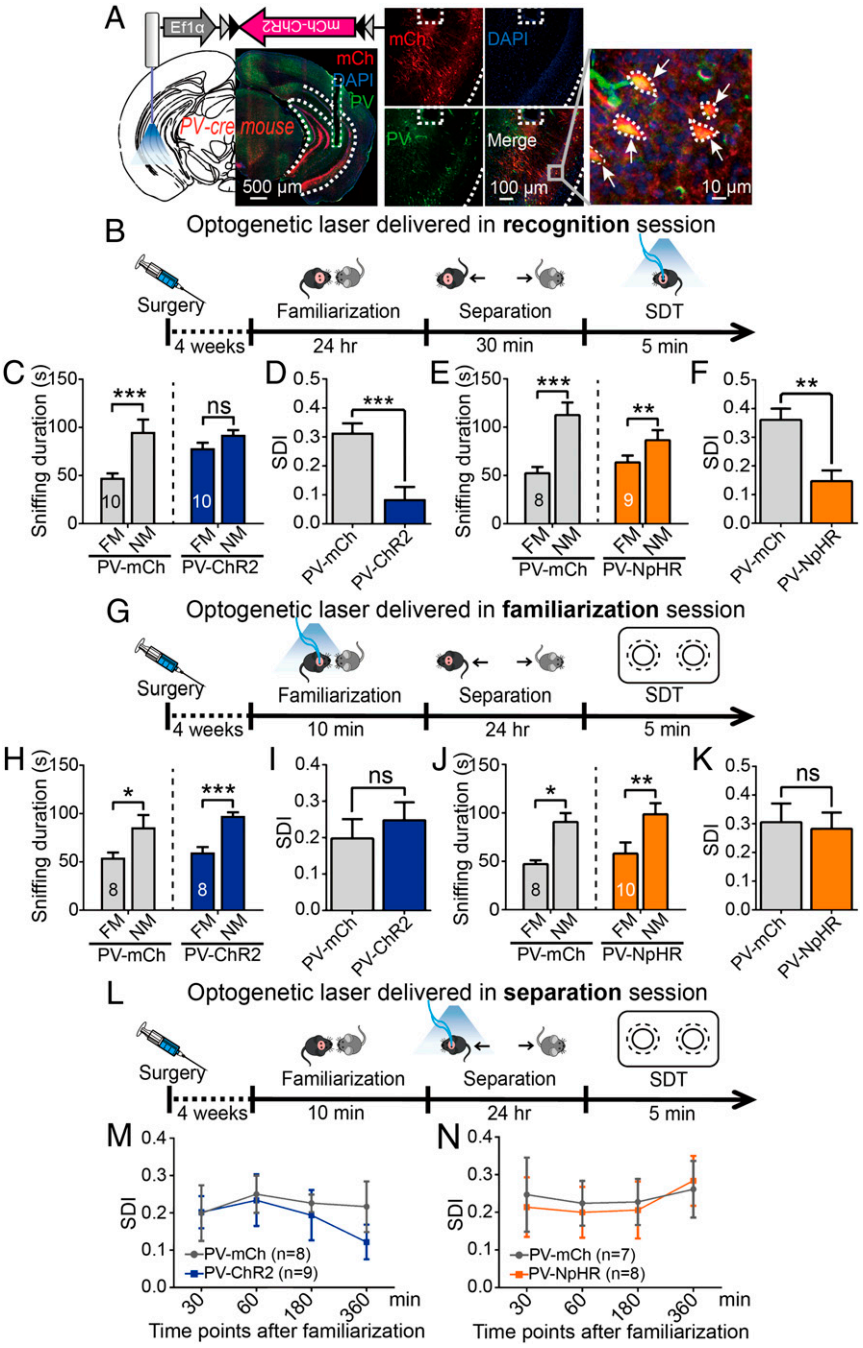

Fig. 3. Selective manipulation of vCA1-PVIs during different stages of social memory. (*A*) Injection of AAV-Ef1α-DIO-hChR2-mCherry or AAV-Ef1α-DIO-eNpHR-GFP into the vCA1 of PV-Cre mice, followed by optical fiber implantation. Representative coronal section shows the expression of ChR2-mCh (red) and their colocalization with PV (green) and DAPI (blue) in the vCA1. (*B–D*) Protocols for optogenetic stimulation of vCA1-PVIs during recognition (*B*), familiarization (*G*), and separation (*L*) sessions. (*C–F*) Sniffing duration (*C*, ChR2, $n = 10$, mCh, $n = 10$; *E*, NpHR, $n = 9$, GFP, $n = 8$) and SDI (*D* and *F*) in the mice with laser stimulation during recognition session. (*H–K*) Sniffing duration (*H*, ChR2, $n = 8$, mCh, $n = 8$; *J*, NpHR, $n = 10$, GFP, $n = 8$) and SDI (*I* and *K*) in the mice with laser stimulation during familiarization session. (*M* and *N*) Line graph delineating the change of SDI when laser stimulation was delivered at different time points during separation session (*M*, mCh, $n = 8$, ChR2: $n = 9$; *N*, GFP, $n = 7$, NpHR, $n = 8$). FM, familiar mouse; NM, novel mouse. The dashed lines outline the subfields of vHPC and the trace of optical fiber in *A* (*Left* and *Middle*); the arrows in A (*Right*) highlight the cells that colocalized with PV and mCh. All data are expressed as mean ± SEM. $^{*}P < 0.05$; $^{**}P < 0.01$; $^{***}P < 0.001$; ns, not significant.

the NpHR mice compared with their control (Fig. 3*N*). Next, we chronically manipulated the vCA1-PVIs of a separate set of mice during the consolidation period through the designer receptor exclusively activated by designer drugs (DREADDs) approach (*SI Appendix*, Fig. S6*A*), in which neuronal activation and inhibition may last 2 to 3 h (33). The results showed that an intraperitoneal (i.p.) injection of clozapine-*N*-oxide (CNO) 3 h after social familiarization did not affect social memory while its administration immediately after familiarization disrupted social discrimination in both AAV-DIO-hM3Dq-mCherry and AAV-DIO-hM4Di-mCherry groups (*SI Appendix*, Fig. S6*B*). These observations imply that PVI presence in the vCA1 is necessary for social memory consolidation, specifically in its early period.

The Activity of vCA1-PVIs Was Dynamically Associated with Social Recognition Processing. We further investigated the potential mechanisms underlying the disruption of discriminatory social behaviors induced by the acute activation and inhibition of vCA1-PVIs during the SDT, in which a pair of familiar or a pair of novel mice were used as the target, and laser stimulation was administered as the subject mice approached one of the targets. The data showed that the ChR2-expressing mice exhibited a significant preference for familiar mice following vCA1-PVI activation while the control group spent a similar amount of time approaching the two familiar mice (Fig. 4*A*). When a pair of novel mice were used as the target, approach-triggered optogenetic excitation did not induce preference or avoidance behaviors in subject mice during the SDT (Fig. 4*C*). These findings indicate that vCA1-PVI hyperactivation at an 8-Hz frequency interrupts social discrimination processes by making subject mice misidentify familiar mice as novel mice and that there is a ceiling effect in sniffing time when activation is coupled with novel mouse investigation. By contrast, in the neuronal inhibition tests, laser stimulation coupled with exploring one of a pair of novel mice or one of a pair of familiar mice did not induce any preference or avoidance behavior during the SDT (Fig. 4 *B* and *D*). Given that social discrimination could be impaired by the optogenetic inhibition of vCA1-PVIs (Fig. 3*F*), no phenotype here suggested that acute suppression of this neuronal population may influence the recall of both familiar and novel social information. Additionally, when the targets were changed to a pair of familiar or novel objects, no effect of vCA1-PVI excitation or inhibition was observed (*SI Appendix*, Fig. S7).

To monitor the natural activities of vCA1-PVIs during social memory's retrieval stage, we injected Cre-dependent AAV vectors carrying the GCaMP6(f) gene into the vCA1s of PV-Cre mice and implanted an optical fiber above the injection site. Before recording began, the fiber was connected to a photometry system through a jumper cable to simultaneous delivery of excitation light and collection of real-time tracking of PV-specific Ca^{2+} transients in SDT (Fig. 5*A*). By aligning the GCaMP signals with video-scored behavioral actions noted in the SDT, we observed behavior-related changes in GCaMP signals across social investigation bouts (Fig. 5*B*). Robust increases in the Ca^{2+} signal usually occurred when subject mice investigated the novel mice while slight Ca^{2+} transients could be elicited by familiar social interaction (Fig. 5 *C* and *D*). Data analysis revealed that interactions with novel mice significantly enhanced bout peaks of Ca^{2+} signals more than interactions with familiar ones did (Fig. 5*E*). When the novel and familiar interaction events were separately distributed into three equal stages (initial, middle, and last stages), we found that the statistical difference between novel and familiar interactions' GCaMP signals disappeared in the last stage (the last 1/3 bouts) (Fig. 5*F*). These findings imply that vCA1-PVI activation associated with novel conspecific exploration decays with social processing. In other words, when a novel target gradually becomes familiar through interaction, PVI activation in the subject diminishes. Further analyses revealed that heading toward novel mice rather than familiar targets enhanced the Ca^{2+} signals of mouse PVIs (Fig. 5 *G*, *I*, and *J*). A single action of heading to the novel mouse without following approach was sometimes sufficient to elicit a Ca^{2+} transient (*SI Appendix*, Fig. S8*A*). By contrast, a withdrawal from the novel mouse induced a sharper and longer reduction in the Ca^{2+} signal than did withdrawal from the familiar one (Fig. 5 *H*, *K*, and *L*). Taken together, our findings suggest that the activation of vCA1-PVIs is more strongly related to the conspecific exploration of novel targets and that the discrimination process occurs before the actual interaction.

To further highlight the role of vCA1-PVIs in social discrimination, we analyzed the changes in Ca^{2+} signals when a subject mouse investigated a familiar mouse, a novel mouse, a toy mouse,

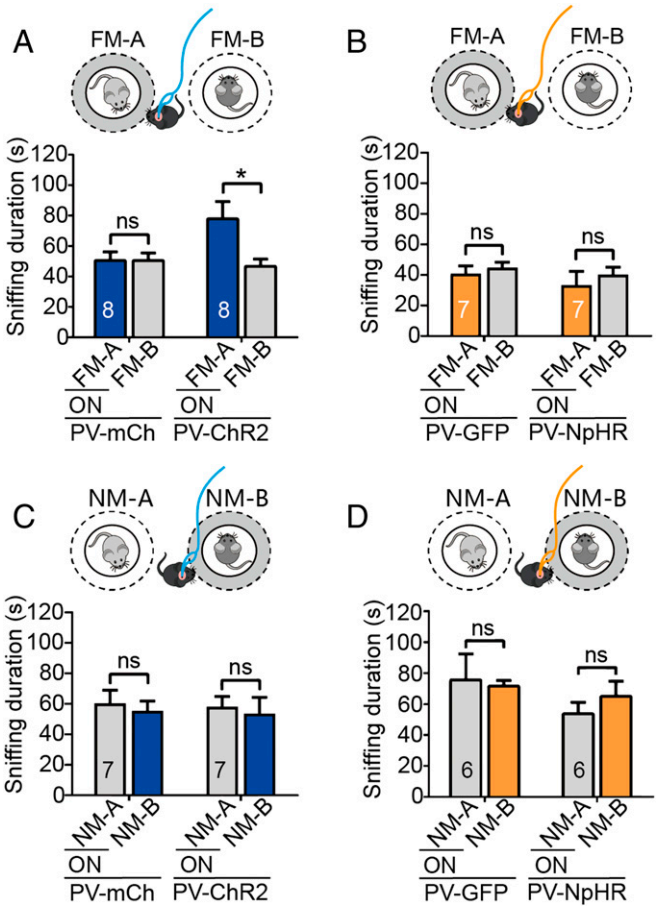

Fig. 4. Effects of optogenetic excitation or inhibition of vCA1-PVIs coupling with investigating one of a pair of familiar/novel mice on social discrimination. (*A* and *B*) When a pair of familiar mice were used as the targets, the time that PV-ChR2 mice ($n = 8$) spent in investigating the familiar mouse (coupling with 473-nm laser stimulation) was enhanced, compared with control mice ($n = 8$) (*A*) while the time that PV-NpHR mice ($n = 7$) spent in investigating the familiar mouse (coupling with 589-nm laser stimulation) was similar to that in control mice ($n = 7$) (*B*). (*C* and *D*) When a pair of novel mice were used as the targets, no significant change of social preference or avoidance was observed in either neuronal excitation (C, mCh, $n = 7$, ChR2: $n = 7$) or inhibition (*D*, GFP, $n = 6$, NpHR, $n = 6$). FM, familiar mouse; NM, novel mouse; ON, turn on the optogenetic laser. All data are expressed as mean ± SEM $^*P < 0.05$; ns, not significant.

and a novel object individually (Fig. 6*A*). These targets were introduced to the subject mouse in a random order. The results revealed that the PV-GCaMP signal substantially increased in response to a novel mouse, resembling the observation made during the SDT, while no marked change was found during investigations of a familiar mouse, novel object, or toy mouse (Fig. 6*B*). The peak of Ca^{2+} signal and latency to reach peak during interactions with novel mice was significantly higher than that during interactions with other targets (Fig. 6 *C* and *D*). We also observed that investigations of the anogenital regions of novel mice exhibited higher peak Ca^{2+} fluorescence in subject mice than did investigations of facial or flank areas (*SI Appendix*, Fig. S8*B*), which indicates the importance of the target's odor information in the discrimination process. This argument is further supported by the following observation: When a toy mouse soaked in urine from a novel mouse was used as a target, a novel mouse-like interaction producing a Ca^{2+} transient occurred, and the signal change decayed rapidly across exploration bouts (*SI Appendix*, Fig. S8*C*). In the control experiment, in which a clean toy mouse was used as a target, the heading action induced a significant increase in the Ca^{2+} signal,

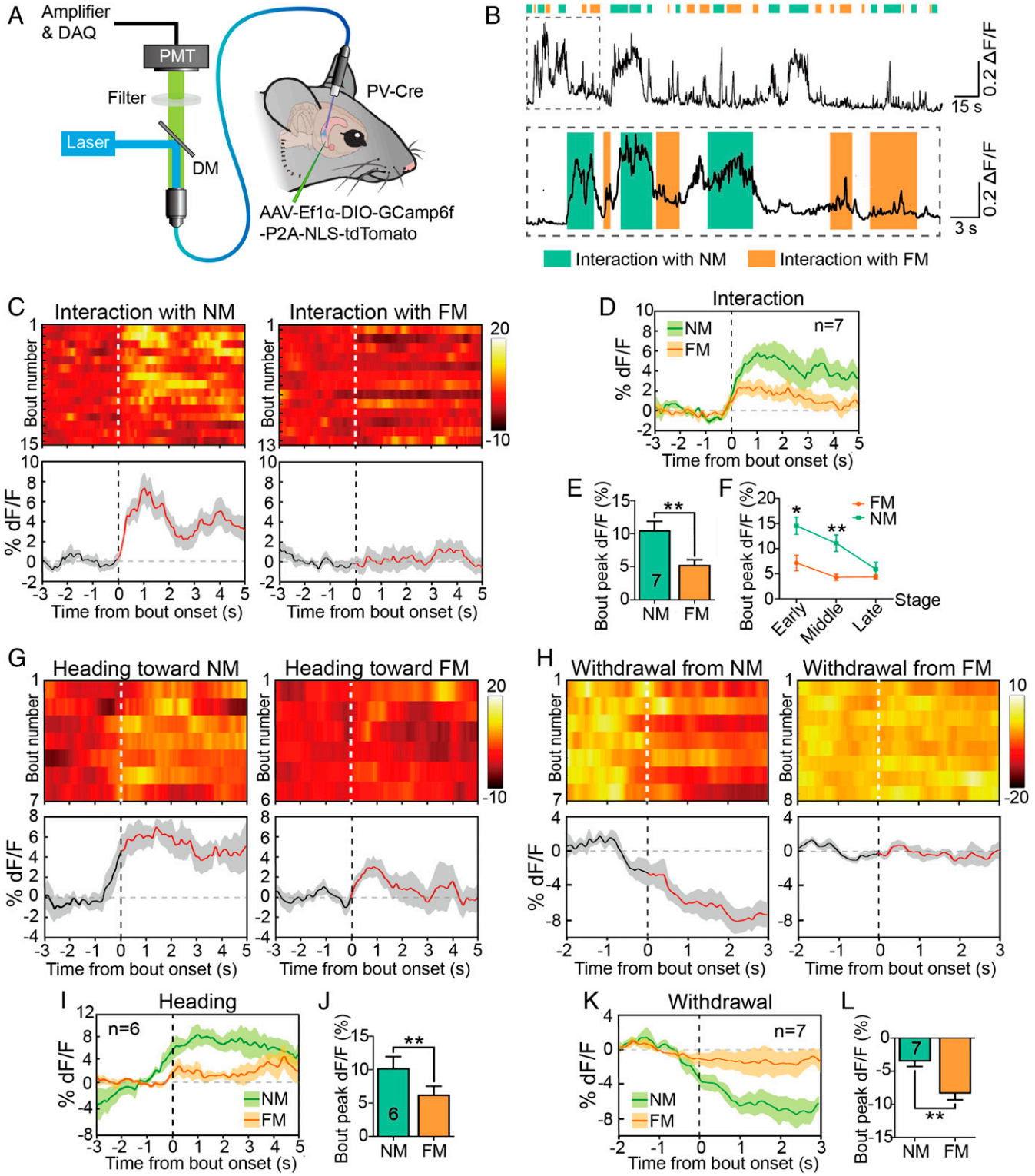

Fig. 5. In vivo measurement of real-time Ca^{2+} dynamics of vCA1-PVIs in freely moving mice in SDT. (*A*) Injection of AAV-Ef1α-DIO-GCaMP6(f)-tdTomato into the vCA1 of PV-Cre mice with an optical fiber implanted above the injection site. (*B*) GCaMP6 signals of vCA1-PVIs during the bouts of social interaction with familiar (orange) or novel mouse (turquoise) in the SDT. (*C*) Heat maps (*Top*) and per-bout stacked plots (*Bottom*) of PV-GCaMP6 signals aligned to start of bout of interaction event. (*D*) Averaged time course of Ca^{2+} transients in freely moving mice ($n = 7$) interacting with a novel or familiar mouse. (*E*) Quantitative analysis of peak dF/F of Ca^{2+} signals when PV-GCaMP6 mice ($n = 7$) interacted with a novel or familiar mouse in SDT. (*F*) When the novel and familiar interaction bouts were separately distributed into three equal stages (initial, middle, and last stages), the statistical difference between novel and familiar interactions' GCaMP signals was shown in the initial and middle stages (the first and second 1/3 bouts). (*G* and *H*) Heat maps (*Top*) and per-bout stacked plots (*Bottom*) of PV-GCaMP6 signals aligned to start of bout of heading toward (*G*) or withdrawal from (*H*) a familiar or novel mouse. (*I and K*) Averaged time course of Ca^{2+} transients in freely moving mice heading toward (*I*, $n = 6$) or withdrew from (*K*, $n = 7$) a novel or familiar mouse. (*J and L*) Quantitative analyses of peak dF/F of Ca^{2+} signals when PV-GCaMP6 mice head to (*J*) or withdrew from (*L*) novel or familiar mouse in SDT. All data are expressed as mean ± SEM. In the time curve graphs, the cloudy area indicates SEM of the averaged data. FM, familiar mouse; NM, novel mouse; DAQ, data acquisition; PMT, photomultiplier tube; DM, dichroic mirror. The dashed lines represent the onset of behavioral bouts. $^{*}P < 0.05$; $^{**}P < 0.01$.

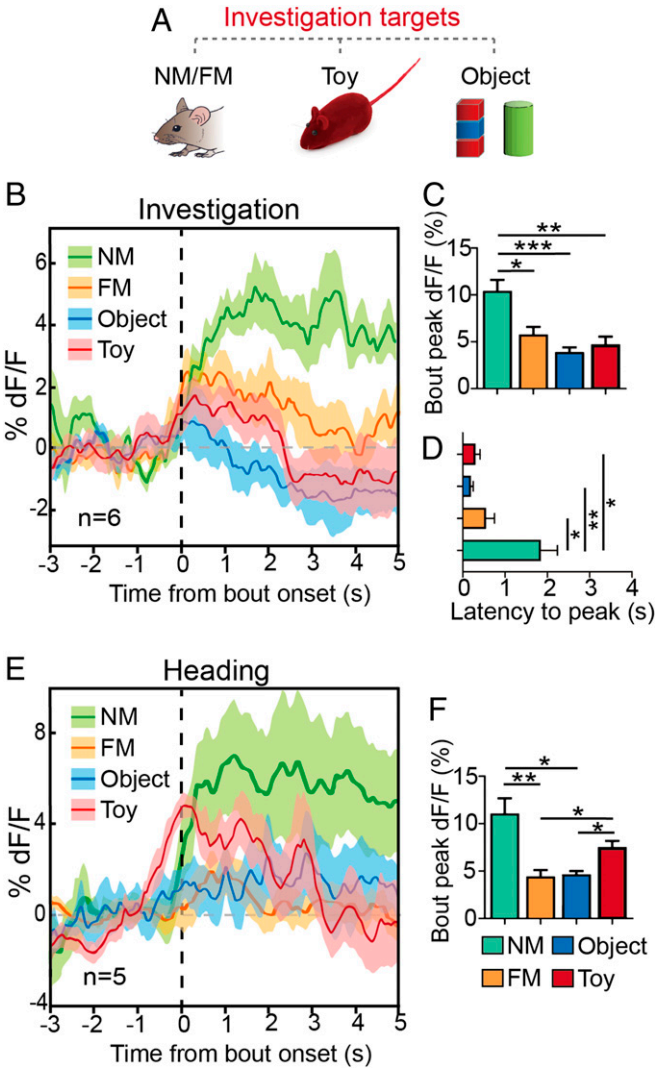

Fig. 6. Real-time Ca^{2+} dynamics of vCA1-PVIs in target investigation. (*A*) Ca^{2+} signals were recorded when a subject mouse investigated a familiar mouse, a novel mouse, a toy mouse, and a novel object individually. (*B*) Averaged time course of Ca^{2+} transients in freely moving mice ($n = 6$) investigating different targets. (*C* and *D*) Quantitative analyses of peak (*C*) and latency to peak (*D*) dF/F of Ca^{2+} signals when PV-GCaMP6 mice investigated different targets. (*E*) Averaged time course of Ca^{2+} transients in freely moving mice ($n = 5$) heading toward different targets. (*F*) Quantitative analysis of peak dF/F of Ca^{2+} signals when PV-GCaMP6 mice head toward different targets. All data are expressed as mean ± SEM. In the time curve graphs, the cloudy area indicates SEM of the averaged data. $^{*}P < 0.05$; $^{**}P < 0.01$; $^{***}P < 0.001$.

which resembled the dynamic and average bout peak during heading toward a novel mouse, indicating that heading-induced Ca^{2+} transients might be driven by the conspecifics-like outward appearance (Fig. 6 *E* and *F*). No significant change in heading action was found in relation to the exploration of the novel object or familiar mouse (Fig. 6*F*).

Finally, to obtain information relating to the different layers of the vCA1 during social discrimination, we analyzed the specific c-Fos expression in the vCA1 of the subject following a 5-min social interaction with a novel or familiar mouse. The subject mice exhibited a greater level of c-Fos expression in the vCA1 when they were exposed to novel mice than when they were exposed to familiar mice (*SI Appendix*, Fig. S9*A*). We classified c-Fos–positive nuclei into three expression levels (low, medium, and high) according to their fluorescent intensities (*SI Appendix*, Fig. S9*B*). Generally, PVIs primarily colocalized with low-expressing (rather than high- or medium-expressing) c-Fos nuclei (*SI Appendix*, Fig. S9*D*). Furthermore, we counted the number of PV^{+} cells distributed in the distinct strata of the vCA1 and found that PV^{+} cells were primarily located in the stratum pyramidale (str. pyr.) (72.1%), the stratum oriens (str. or.; 24.9%), and, rarely, in more superficial strata, such as the stratum radiatum (str. rad.) (4%) (*SI Appendix*, Fig. S9*C*). Further analyses revealed that, in the str. pyr. but not the str. or., the PVIs of mice in the novel-interaction group showed a higher proportion of colocalization with low-expressing c-Fos than did the familiar-interaction group (*SI Appendix*, Fig. S9 *E* and *F*). These data provide evidence that PVI activity in the str. pyr. of the vCA1 is vital for distinguishing between novel and familiar conspecifics.

Discussion

In this work, we demonstrated that PVIs in the vCA1 are specifically engaged in subjects' social information retrieval but not its encoding. Moreover, we revealed that the activation of vCA1-PVIs was important in helping mice discriminate between novel and familiar conspecifics. This study explores the involvement of nonprincipal neurons in the hippocampus during specific processing stages in social memory functions, thus attempting to elucidate how hippocampal interneurons and local microcircuits participate in this cognitive process.

Two months of social isolation impaired the social discrimination functions of mice and selectively reduced the number of PV-immunoreactive cells in their vHPCs. In particular, social isolation-induced changes in PV expression in the vCA1 covaried with SDT performance. Social isolation has been proven to influence neuroplasticity-related biomarkers in the hippocampus (34–36). Reduced numbers of PVIs in the vCA1 might reflect the plasticity of social memory-related networks as a response to chronic inactivation, which in turn leads to failure to discriminate between novel and familiar mice. However, this explanation may be insufficient because long-term social isolation is also a type of chronic stress (37) and induces multiple alterations in the neural system, such as increased oxidative stress (27, 28, 38) and the down-regulation of brain-derived neurotrophic factor (36, 39). Nevertheless, these results are indicative of potential associations between vCA1-PVIs and social memory performance.

Through a TeNT-mediated blockade of the synaptic transmission of vCA1-PVIs, we attempted to identify the causal relationship between vCA1-PVIs and social memory. This manipulation simulated the chronic impairment of PVIs in psychiatric diseases (40–42) and resulted in a marked disruption in social recognition memory similar to that observed in models of schizophrenia (11, 14) and Alzheimer's disease (12). SOMIs, another important subtype of inhibitory interneurons in the hippocampus, make up ∼12% of all GABAergic cells in the vCA1 (43). The results of this study indicate that vCA1-SOMIs do not appear to engage in social memory processes. Hippocampal PVIs are more responsible for higher cognitive functions than are SOMIs (44, 45). This functional distinction between the roles of SOMIs and PVIs in the vCA1 may be based on differences in the distribution of layers and morphological and electrophysiological properties (15, 17, 43, 46–48). Although both subtypes of interneurons exhibit inhibitory control over PCs, hippocampal PVIs and SOMIs may play different roles in the management of local circuits and synergizing oscillation (24, 47, 49, 50).

PVIs have functions in intrinsic rhythm generation and hippocampal PC coordination (22–24). Recent work by Okuyama et al. (7) has demonstrated the critical roles of vCA1-PCs in the deep sublayers of the str. pyr. (closer to the str. or.) and the shell projection of the nucleus accumbens (NAc) for purposes of encoding and retrieving social memory. The hyperactivation of the PCs in the vCA1 disrupted social memory processes during

the SDT by making the subjects identify novel mice as familiar mice (7). Our study also revealed that the hyperexcitability of vCA1-PVIs impaired subject social discrimination ability as they perceived familiar mice to be novel mice. In fact, PVIs preferentially target PCs located in the deep layers over those in the superficial (closer to the str. rad.) sublayers of the str. pyr. of the hippocampal CA1 subfield (50), which are the same sublayers from which the vCA1-NAc shell pathway originates (7). Under natural conditions, PVIs demonstrated a higher level of excitation when PV-GCaMP6 mice were exposed to novel mice than to familiar ones. An analysis of c-Fos supported the results from Ca^{2+} imaging and provided further evidence that PVIs in the str. pyr. may be more involved in this social process than those in the str. or. As PVIs exert powerful inhibitory control over the local network and the output of projection neurons (24, 50), it is probable that the artificial excitation of PVIs suppresses the engram neurons that store social information about familiar individuals while the artificial silencing of PVIs by NpHR or TeNT overexcites the large population of vCA1 pyramidal cells by disinhibiting local circuits. All these manipulations interfere with the normal functions of the hippocampal network and therefore result in a failure to socially discriminate. Specifically, theta wave rhythmicity has been demonstrated in association with novelty stimulation during social interactions (51). We stimulated hippocampal PVIs at the frequency of a theta rhythm (8 Hz), a frequency at which the hippocampal PC network and intrinsic hippocampal oscillations are powerfully controlled (24, 52). Additionally, our results indicate that stimulating vCA1-PVIs at a low gamma wave frequency (40 Hz) could block subjects' abilities to recognize conspecifics in an SDT and elicit a significant preference for "laser on" one of a pair of familiar mice (*SI Appendix*, Fig. S10). These results also suggest that the gamma oscillation modulated by PVIs may be also involved in social discrimination (53). Although a recent study indicated that exciting cortical PVIs in a theta-gamma nested pattern (40 Hz nested at 8 Hz) could reverse social novelty deficits in autism-like animals (53), how the hippocampal network modulated by PVIs participates in social memory retrieval must be further explored.

It is also notable that, although reduced SDI scores suggest a decline in subject abilities to recall social memory, PVI inhibition through optogenetic stimulation did not completely block social discrimination in the SDT. This differed from the result obtained with the TeNT mice. Behavioral differences between optogenetic-manipulated and TeNT-lesion mice were also observed in the SDT (with roommates) and the NORT. Given that hippocampal PVIs were demonstrated to be important in synaptic plasticity (20, 21), hippocampal neurogenesis (54, 55), and amyloid load reduction (56), it is reasonable to speculate that a difference exists between chronic lesions and acute modulation. A similar phenomenon has been observed in the medial prefrontal cortex: Optogenetic manipulation and the TeNT-induced functional removal of PVIs exerted different effects on social novelty recognition (53, 57). The present findings indicate that the chronic functional loss of vCA1-PVIs through certain mechanisms not only impairs the subject's long-term social recognition memory, but also disrupts their entire recognition ability (21, 52, 58, 59). Additionally, TeNT-mediated chronic lesions on vCA1-PVIs may also affect social memory's consolidation process, as was revealed in the DREADD experiments detailed here. Previous studies have shown that administrating CNO to suppress dCA1-PVIs immediately after shock-cue association could block fear memory consolidation (52, 59), indicating that hippocampal PVIs have a role in episodic memory consolidation, especially in its early stage. How vCA1-PVIs work during the consolidation period of social memory must be investigated further.

The CA1 innervates multiple brain regions (60). There is substantial evidence confirming that the dCA1 and vCA1 subregions are dissociable through neural connection, thus underlining their functional separation (60, 61). The vCA1 was recently highlighted for playing an essential role in social discrimination while the dCA1 was found to engage more preferentially in nonsocial discrimination (7, 62). Similarly, we found that PVIs in the vCA1, but not in the dCA1, are particularly involved in social memory, suggesting a subregionally dependent function in memory modulation within nonprincipal cells. Although we did not observe any change in the dCA2-PVIs of socially isolated mice, the role of the dCA2 in modulating social memory cannot be neglected (8, 10, 14, 62). In some disease models, reduced PVI density in the dCA2 has been detected and is linked to social memory deficits (12, 14, 63). Functional damages in different subfields in hippocampus (e.g., dCA2 and vCA1) may be involved in different disease and stressed animal models. Previous demonstrations that the connections between the dCA2 and vCA1 in the hippocampus are important to social memory support this implication (62).

In summary, our study reveals that PVIs in the vCA1 play the role of a discriminator in social memory-related networks and that their activity is essential for distinguishing novel conspecifics from familiar ones, which highlights the importance of hippocampal interneurons in social memory. These findings could be instrumental in understanding the neuropathological mechanisms underlying the aberrant social memory functions present in multiple psychiatric disorders.

Materials and Methods

Animals. PV- and SOM-IRES-Cre mice were primarily imported from The Jackson Laboratory. All mice were maintained within a controlled environment (23 ± 1 °C; 12-h light/dark cycle) with food and water available ad libitum. All experimental procedures were conducted in accordance with the regulations of the Laboratory of Animal Care and Use Committees of the Institute of Psychology, Chinese Academy of Sciences.

Virus Preparation and Stereotaxic Surgery. All recombinant AAV vectors comprised a Double-Floxed Inverted Open (DIO) reading frame construct, which led to a Cre-dependent expression strategy. The injection sites were the vCA1 (anteroposterior [AP]: −3.16 mm; mediolateral [ML]: ±3.20 mm; dorsoventral [DV]: −4.50 mm) and the dCA1 (AP: −2.00 mm; ML: ±1.50 mm; DV: −1.50 mm). Optical fibers were implanted 0.5 mm above injection sites. In the in vivo Ca^{2+} photometry experiment, optical fibers were implanted 0.1 mm above the virus injection site. Following the surgery, the animals recovered for 3 to 4 wk before experimentation began.

Optogenetic Manipulations and Behavioral Tests. PVIs were activated using a 473-nm blue laser (20 ms per pulse, 8 Hz, 15 mW) or inhibited by a 589-nm yellow laser (constant, 10 mW). The following tests were performed: an SDT, a three-chamber sociality test, a NORT, an EPM, an open field test, and a PPI test. The three-chamber sociality test, the EPM, and the open field test were analyzed using the Xeye Aba tracking system (Beijing Macroambitior S&T Development Co., Ltd.) while the SDT and NORT were analyzed by a well-trained observer who was blinded to the groups.

Chemogenetical Manipulation. PV-hM3Dq and PV-mCh mice were injected with CNO (HY-17366; MedChemExpress) intraperitoneally (10 mg/kg) immediately or 3 h after a familiarization session. PV-hM4Di mice received 5 mg/kg CNO; they became seizure-susceptible at a dose of 10 mg/kg. Mice exhibiting seizure behaviors were excluded from the study.

In Vivo Ca^{2+} Fiber Photometry. A commercialized fiber photometry system (ThinkerTech Inc.) was used to record the Ca^{2+} signals from the PVIs. The fluorescence signals were normalized within each mouse by calculating the delta fluorescence/fluorescence (dF/F) as $(F - F_0)/F_0$, where F_0 is the baseline fluorescence signal averaged over 3 s (heading and interaction) or 2 s (withdrawal) before the onset of the behavioral event.

Immunohistochemistry. Mice were perfused with a 4% paraformaldehyde (PFA) solution. Brains were equilibrated with 30% sucrose and were then cryosectioned. After blocking, the sections were incubated overnight with primary antibodies; this was followed by a 2-h incubation period with secondary antibodies. The sections were then mounted onto slides and imaged through fluorescence microscopy (DM5500B; Leica).

Statistics. The results are expressed as mean ± SEM. Data were evaluated via a *t* test, Mann–Whitney *U* test, or analysis of variance (ANOVA), and evaluations were followed by Bonferroni's post hoc test. The criterion for statistical significance was $P < 0.05$.

For full detailed materials and methods, see *SI Appendix, SI Methods*.

ACKNOWLEDGMENTS. This work was supported by National Natural Science Foundation of China Grants 31571108 and 31371038, Beijing Natural Science Foundation Grant 5162023, National Key Basic Research Program of China Grant 2015CB553501, and Key Laboratory of Mental Health, Institute of Psychology, Chinese Academy of Sciences.

1. T. Okuyama, Social memory engram in the hippocampus. *Neurosci. Res.* **129**, 17–23 (2018).
2. S. Daumas, H. Halley, B. Francés, J. M. Lassalle, Encoding, consolidation, and retrieval of contextual memory: Differential involvement of dorsal CA3 and CA1 hippocampal subregions. *Learn. Mem.* **12**, 375–382 (2005).
3. M. F. Carr, S. P. Jadhav, L. M. Frank, Hippocampal replay in the awake state: A potential substrate for memory consolidation and retrieval. *Nat. Neurosci.* **14**, 147–153 (2011).
4. N. Burgess, E. A. Maguire, J. O'Keefe, The human hippocampus and spatial and episodic memory. *Neuron* **35**, 625–641 (2002).
5. J. H. Kogan, P. W. Frankland, A. J. Silva, Long-term memory underlying hippocampus-dependent social recognition in mice. *Hippocampus* **10**, 47–56 (2000).
6. A. Montagrin, C. Saiote, D. Schiller, The social hippocampus. *Hippocampus* **28**, 672–679 (2018).
7. T. Okuyama, T. Kitamura, D. S. Roy, S. Itohara, S. Tonegawa, Ventral CA1 neurons store social memory. *Science* **353**, 1536–1541 (2016).
8. F. L. Hitti, S. A. Siegelbaum, The hippocampal CA2 region is essential for social memory. *Nature* **508**, 88–92 (2014).
9. E. L. Stevenson, H. K. Caldwell, Lesions to the CA2 region of the hippocampus impair social memory in mice. *Eur. J. Neurosci.* **40**, 3294–3301 (2014).
10. A. S. Smith, S. K. Williams Avram, A. Cymerblit-Sabba, J. Song, W. S. Young, Targeted activation of the hippocampal CA2 area strongly enhances social memory. *Mol. Psychiatry* **21**, 1137–1144 (2016).
11. A. Becker, G. Grecksch, Social memory is impaired in neonatally ibotenic acid lesioned rats. *Behav. Brain Res.* **109**, 137–140 (2000).
12. R. M. Deacon, E. Koros, K. D. Bornemann, J. N. Rawlins, Aged Tg2576 mice are impaired on social memory and open field habituation tests. *Behav. Brain Res.* **197**, 466–468 (2009).
13. H. Higashida *et al*., Social memory, amnesia, and autism: Brain oxytocin secretion is regulated by NAD+ metabolites and single nucleotide polymorphisms of CD38. *Neurochem. Int.* **61**, 828–838 (2012).
14. R. A. Piskorowski *et al*., Age-dependent specific changes in area CA2 of the hippocampus and social memory deficit in a mouse model of the 22q11.2 deletion syndrome. *Neuron* **89**, 163–176 (2016).
15. T. Klausberger, P. Somogyi, Neuronal diversity and temporal dynamics: The unity of hippocampal circuit operations. *Science* **321**, 53–57 (2008).
16. H. Hu, J. Gan, P. Jonas, Interneurons. Fast-spiking, parvalbumin^{+} GABAergic interneurons: From cellular design to microcircuit function. *Science* **345**, 1255263 (2014).
17. A. Kepecs, G. Fishell, Interneuron cell types are fit to function. *Nature* **505**, 318–326 (2014).
18. R. Tremblay, S. Lee, B. Rudy, GABAergic interneurons in the neocortex: From cellular properties to circuits. *Neuron* **91**, 260–292 (2016).
19. M. J. Bezaire, I. Soltesz, Quantitative assessment of CA1 local circuits: Knowledge base for interneuron-pyramidal cell connectivity. *Hippocampus* **23**, 751–785 (2013).
20. O. Caillard *et al*., Role of the calcium-binding protein parvalbumin in short-term synaptic plasticity. *Proc. Natl. Acad. Sci. U.S.A.* **97**, 13372–13377 (2000).
21. F. Donato, S. B. Rompani, P. Caroni, Parvalbumin-expressing basket-cell network plasticity induced by experience regulates adult learning. *Nature* **504**, 272–276 (2013).
22. J. A. Cardin *et al*., Driving fast-spiking cells induces gamma rhythm and controls sensory responses. *Nature* **459**, 663–667 (2009).
23. V. S. Sohal, F. Zhang, O. Yizhar, K. Deisseroth, Parvalbumin neurons and gamma rhythms enhance cortical circuit performance. *Nature* **459**, 698–702 (2009).
24. B. Amilhon *et al*., Parvalbumin interneurons of hippocampus tune population activity at theta frequency. *Neuron* **86**, 1277–1289 (2015).
25. D. Zou *et al*., DREADD in parvalbumin interneurons of the dentate gyrus modulates anxiety, social interaction and memory extinction. *Curr. Mol. Med.* **16**, 91–102 (2016).
26. H. Shahar-Gold, R. Gur, S. Wagner, Rapid and reversible impairments of short- and long-term social recognition memory are caused by acute isolation of adult rats via distinct mechanisms. *PLoS One* **8**, e65085 (2013).
27. H. Ueno *et al*., Region-specific impairments in parvalbumin interneurons in social isolation-reared mice. *Neuroscience* **359**, 196–208 (2017).
28. Z. Jiang, G. R. Rompala, S. Zhang, R. M. Cowell, K. Nakazawa, Social isolation exacerbates schizophrenia-like phenotypes via oxidative stress in cortical interneurons. *Biol. Psychiatry* **73**, 1024–1034 (2013).
29. C. Bloomfield *et al*., Chandelier cartridges in the prefrontal cortex are reduced in isolation reared rats. *Synapse* **62**, 628–631 (2008).
30. S. S. Kaalund *et al*., Differential expression of parvalbumin in neonatal phencyclidine-treated rats and socially isolated rats. *J. Neurochem.* **124**, 548–557 (2013).
31. D. Filipović, J. Zlatković, P. Gass, D. Inta, The differential effects of acute vs. chronic stress and their combination on hippocampal parvalbumin and inducible heat shock protein 70 expression. *Neuroscience* **236**, 47–54 (2013).
32. M. Engelmann, J. Hädicke, J. Noack, Testing declarative memory in laboratory rats and mice using the nonconditioned social discrimination procedure. *Nat. Protoc.* **6**, 1152–1162 (2011).
33. B. L. Roth, DREADDs for neuroscientists. *Neuron* **89**, 683–694 (2016).
34. A. Djordjevic, M. Adzic, J. Djordjevic, M. B. Radojcic, Chronic social isolation is related to both upregulation of plasticity genes and initiation of proapoptotic signaling in Wistar rat hippocampus. *J. Neural Transm. (Vienna)* **116**, 1579–1589 (2009).
35. J. Djordjevic, A. Djordjevic, M. Adzic, M. B. Radojcic, Effects of chronic social isolation on Wistar rat behavior and brain plasticity markers. *Neuropsychobiology* **66**, 112–119 (2012).
36. A. Ieraci, A. Mallei, M. Popoli, Social isolation stress induces anxious-depressive-like behavior and alterations of neuroplasticity-related genes in adult male mice. *Neural Plast.* **2016**, 6212983 (2016).
37. P. Steullet *et al*., Oxidative stress-driven parvalbumin interneuron impairment as a common mechanism in models of schizophrenia. *Mol. Psychiatry* **22**, 936–943 (2017).
38. S. Schiavone *et al*., Involvement of NOX2 in the development of behavioral and pathologic alterations in isolated rats. *Biol. Psychiatry* **66**, 384–392 (2009).
39. R. M. Barrientos *et al*., Brain-derived neurotrophic factor mRNA downregulation produced by social isolation is blocked by intrahippocampal interleukin-1 receptor antagonist. *Neuroscience* **121**, 847–853 (2003).
40. D. R. Brady, E. J. Mufson, Parvalbumin-immunoreactive neurons in the hippocampal formation of Alzheimer's diseased brain. *Neuroscience* **80**, 1113–1125 (1997).
41. Z. J. Zhang, G. P. Reynolds, A selective decrease in the relative density of parvalbumin-immunoreactive neurons in the hippocampus in schizophrenia. *Schizophr. Res.* **55**, 1–10 (2002).
42. D. J. Lodge, M. M. Behrens, A. A. Grace, A loss of parvalbumin-containing interneurons is associated with diminished oscillatory activity in an animal model of schizophrenia. *J. Neurosci.* **29**, 2344–2354 (2009).
43. T. Kosaka, J. Y. Wu, R. Benoit, GABAergic neurons containing somatostatin-like immunoreactivity in the rat hippocampus and dentate gyrus. *Exp. Brain Res.* **71**, 388–398 (1988).
44. H. T. Chao *et al*., Dysfunction in GABA signalling mediates autism-like stereotypies and Rett syndrome phenotypes. *Nature* **468**, 263–269 (2010).
45. A. Ito-Ishida, K. Ure, H. Chen, J. W. Swann, H. Y. Zoghbi, Loss of MeCP2 in parvalbumin- and somatostatin-expressing neurons in mice leads to distinct rett syndrome-like phenotypes. *Neuron* **88**, 651–658 (2015).
46. T. Kosaka, H. Katsumaru, K. Hama, J. Y. Wu, C. W. Heizmann, GABAergic neurons containing the Ca2+-binding protein parvalbumin in the rat hippocampus and dentate gyrus. *Brain Res.* **419**, 119–130 (1987).
47. T. Klausberger *et al*., Brain-state- and cell-type-specific firing of hippocampal interneurons in vivo. *Nature* **421**, 844–848 (2003).
48. I. Katona, L. Acsády, T. F. Freund, Postsynaptic targets of somatostatin-immunoreactive interneurons in the rat hippocampus. *Neuroscience* **88**, 37–55 (1999).
49. R. N. Leão *et al*., OLM interneurons differentially modulate CA3 and entorhinal inputs to hippocampal CA1 neurons. *Nat. Neurosci.* **15**, 1524–1530 (2012).
50. S. H. Lee *et al*., Parvalbumin-positive basket cells differentiate among hippocampal pyramidal cells. *Neuron* **82**, 1129–1144 (2014).
51. A. Tendler, S. Wagner, Different types of theta rhythmicity are induced by social and fearful stimuli in a network associated with social memory. *eLife* **4**, e03614 (2015).
52. N. Ognjanovski *et al*., Parvalbumin-expressing interneurons coordinate hippocampal network dynamics required for memory consolidation. *Nat. Commun.* **8**, 15039 (2017).
53. W. Cao *et al*., Gamma oscillation dysfunction in mPFC leads to social deficits in neuroligin 3 R451C knockin mice. *Neuron* **97**, 1394 (2018).
54. J. Song *et al*., Parvalbumin interneurons mediate neuronal circuitry-neurogenesis coupling in the adult hippocampus. *Nat. Neurosci.* **16**, 1728–1730 (2013).
55. H. Bao *et al*., Long-range GABAergic inputs regulate neural stem cell quiescence and control adult hippocampal neurogenesis. *Cell Stem Cell* **21**, 604–617.e5 (2017).
56. H. F. Iaccarino *et al*., Gamma frequency entrainment attenuates amyloid load and modifies microglia. *Nature* **540**, 230–235 (2016).
57. A. J. Murray *et al*., Parvalbumin-positive interneurons of the prefrontal cortex support working memory and cognitive flexibility. *Sci. Rep.* **5**, 16778 (2015).
58. G. Çaliskan *et al*., Identification of parvalbumin interneurons as cellular substrate of fear memory persistence. *Cereb. Cortex* **26**, 2325–2340 (2016).
59. F. Xia *et al*., Parvalbumin-positive interneurons mediate neocortical-hippocampal interactions that are necessary for memory consolidation. *eLife* **6**, e27868 (2017).
60. S. Ciocchi, J. Passecker, H. Malagon-Vina, N. Mikus, T. Klausberger, Brain computation. Selective information routing by ventral hippocampal CA1 projection neurons. *Science* **348**, 560–563 (2015).
61. Y. Yang, J. Z. Wang, From structure to behavior in basolateral amygdala-Hippocampus circuits. *Front. Neural Circuits* **11**, 86 (2017).
62. T. Raam, K. M. McAvoy, A. Besnard, A. H. Veenema, A. Sahay, Hippocampal oxytocin receptors are necessary for discrimination of social stimuli. *Nat. Commun.* **8**, 2001 (2017).
63. F. M. Benes, E. W. Kwok, S. L. Vincent, M. S. Todtenkopf, A reduction of nonpyramidal cells in sector CA2 of schizophrenics and manic depressives. *Biol. Psychiatry* **44**, 88–97 (1998).